

Tumor-infiltrating M2 macrophages driven by specific genomic alterations are associated with prognosis in bladder cancer

YONGPING XUE*, LIPING TONG*, FEI LIU*, ANWEI LIU, SHUXIONG ZENG,
QIAO XIONG, ZEYU YANG, XING HE, YINGHAO SUN and CHUANLIANG XU

Department of Urology, Changhai Hospital, Second Military Medical University, Shanghai 200433, P.R. China

Received November 17, 2018; Accepted May 30, 2019

DOI: 10.3892/or.2019.7196

Abstract. The present study aimed to explore the mechanism by which the immune landscape of the tumor microenvironment influences bladder cancer. CIBERSORT and ssGSEA analyses revealed that M2 macrophages accounted for the highest proportion from 22 subsets of tumor-infiltrating immune cells and were enriched in higher histologic grade and higher pathologic stage bladder cancer and 'basal' subtype of muscle invasive bladder cancer (MIBC). Kaplan-Meier survival curve analysis indicated that patients with high numbers of infiltrating M2 macrophages had worse overall and disease-specific survival rates. RNA sequencing and immunohistochemistry results indicated that M2 macrophages were enriched in MIBC and promoted angiogenesis. M2 macrophage infiltration was higher in bladder cancer tissues with mutant TP53, RB transcriptional corepressor 1, phosphatidylinositol-4,5-bisphosphate 3-kinase catalytic subunit α , lysine methyltransferase 2A, lysine demethylase 6A and apolipoprotein B mRNA editing enzyme catalytic-poly-peptide-like, but lower in tissues with mutant fibroblast

growth factor receptor 3 (FGFR3), E74-like ETS transcription factor 3, PC4 and SFRS1 interacting protein 1 and transmembrane and coiled-coil domains 4. In addition, M2 macrophage infiltration was lower in the tissues with amplified FGFR3, erb-b2 receptor tyrosine kinase 2, BCL2-like 1, telomerase reverse transcriptase and tyrosine-3-monooxygenase/tryptophan-5-monooxygenase activation protein ζ , as well as in the tissues with deleted cyclin-dependent kinase inhibitor 2A, CREB binding protein, AT-rich interaction domain 1A, fragile histidine triad diadenosine triphosphatase, phosphodiesterase 4D, RAD51 paralog B, nuclear receptor corepressor 1 and protein tyrosine phosphatase receptor type D. Finally, seven micro (mi) RNAs (miR-214-5p, miR-223-3p, miR-155-5p, miR-199a-3p, miR-199b-3p, miR-146b-5p, miR-142-5p) which were expressed differentially in at least three mutant genes and were positively correlated with M2 macrophage infiltration as well as expressed highly in high grade bladder cancer were identified. Overall, the present study concluded that M2 macrophages are the predominant tumor-infiltrating immune cell in bladder cancer and differentially expressed miRNAs due to cancer-specific genomic alterations may be important drivers of M2 macrophage infiltration. These findings suggested that M2 macrophage infiltration may serve as a potential immunotherapy target in bladder cancer.

Correspondence to: Professor Chuanliang Xu or Dr Yinghao Sun, Department of Urology, Changhai Hospital, Second Military Medical University, 168 Changhai Road, Shanghai 200433, P.R. China
E-mail: xuchuanliang@vip.126.com
E-mail: sunyinghao@smmu.edu.cn

*Contributed equally

Abbreviations: NMIBC, non-muscle invasive bladder cancer; MIBC, muscle invasive bladder cancer; TCGA, The Cancer Genome Atlas; TME, tumor microenvironment; NKs, natural killer cells; TAMs, tumor-associated macrophages; Tregs, regulatory T cells; GEO, Gene Expression Omnibus; EBI, European Bioinformatics Institute; ssGSEA, single-sample geneset enrichment analysis; CIBERSORT, Cell Type Identification By Estimating Relative Subsets Of known RNA Transcripts; RNA-seq, RNA sequencing; TIDCs, tumor-infiltrating dendritic cells; TILs, tumor-infiltrating lymphocytes

Key words: tumor microenvironment, tumor-infiltrating immune cell, tumor-associated macrophage, genomics, bladder cancer

Introduction

Bladder cancer is the 9th most common and the 13th most fatal type of cancer worldwide (1). Approximately 75% of patients with bladder cancer have non-muscle invasive bladder cancer (NMIBC) and ~25% have muscle invasive bladder cancer (MIBC) or metastatic disease at the time of initial diagnosis (2,3). Different molecular subtypes of bladder cancer have unique clinical characteristics and therapeutic responses. For instance, patients with 'basal' subtype of MIBC are known to have shorter disease-specific survival and overall survival rate (4,5). MIBC is a highly lethal disease and its overall five-year survival rate is 30-50%, whereas that for metastatic bladder cancer is 5% (3,6).

The tumor microenvironment (TME) consists predominantly of tumor cells, stroma and infiltrating immune cells. Immune cells in the TME may exert either tumor-suppressive or tumor-promoting effects. CD8⁺ T cells and natural killer cells (NKs) mediate antitumor functions, whereas tumor-associated

macrophages (TAMs) and regulatory T cells (Tregs) serves as tumor-promoting agents (7,8). As an important component of the innate and adaptive immunity, macrophages may polarize into different functional phenotypes, such as the classically activated M1 and the alternatively activated M2 macrophages, depending on the external stimulus (9). Increasing evidence suggests that M2 macrophages could perform immunosuppressive functions and promote tumor progression and metastasis (7,10-12). It is therefore speculated that the M2 macrophages may have potential as immunotherapy targets (7).

Recently, immunotherapy based on immune checkpoint inhibitors has achieved satisfactory results in the treatment of bladder cancer. However, this outcome was limited to only a subset of patients, since others failed to respond to this therapy (13). Hence, it is important to determine the essential immune components and relevant mechanisms that affect tumor progression in order to improve the immunotherapy of bladder cancer.

The majority of previous studies on the TME associated with bladder cancer have mainly focused on a few types of immune cells and were performed on small numbers of samples (14,15). There is no large-scale data based on big numbers of samples to identify important immune components in bladder cancer. To the best of our knowledge, the molecular mechanisms of immune activities in the bladder cancer microenvironment have not been sufficiently researched.

The present study aimed to explore the predominant tumor-infiltrating immune cell subsets in the bladder cancer microenvironment and the signals recruiting them. Bioinformatics methods were employed to analyze the immune infiltration profile and revealed that M2 macrophage infiltration levels were associated with the histologic grade, pathologic stage, and worse survival in bladder cancer. Bladder cancer-specific genomic alterations, such as gene mutation and copy number alterations, may be important drivers of M2 macrophage infiltration.

Materials and methods

Gene expression datasets. The gene expression dataset (426 samples) and microRNA (miRNA) mature strand expression dataset (429 samples), based on RNA sequencing (RNA-seq) data from The Cancer Genome Atlas (TCGA) bladder urothelial carcinoma cohort, were downloaded from the University of California Santa Cruz (UCSC) xena browser (<https://xenabrowser.net/datapages/>). The gene expression data were presented as $\log_2(x+1)$ -transformed RNA-seq by expectation maximization (RSEM)-normalized count values derived from TCGA level 3 data, and miRNA mature strand expression data were presented as $\log_2(\text{RPM}+1)$ -transformed reads-per-million (RPM) values derived from TCGA level 3 data. The gene expression validation datasets were downloaded from Gene Expression Omnibus (GEO) database (<https://www.ncbi.nlm.nih.gov/geo/>) and European Bioinformatics Institute (EBI) ArrayExpress (<https://www.ebi.ac.uk/arrayexpress/>). The expression dataset of 224 samples in GSE32894, expression dataset of 142 samples in GSE48277, and dataset of 85 samples in E-MTAB-1803 were analyzed to confirm the results derived from the analyses of TCGA

dataset in the present study. All expression data was provided as normalized data, after performing \log_2 conversion on GSE32894 and E-MTAB-1803 datasets.

Clinical data. Clinical data of TCGA dataset were downloaded from the UCSC Xena browser, including histologic grade, pathologic stage and survival information for patients with bladder cancer. The molecular subtype information of TCGA samples was obtained from the supplementary file of the MIBC Molecular Characterization reported by Robertson *et al* (3). Clinical data for GSE32894, GSE48277 and E-MTAB-1803 datasets were obtained from GEO and EBI ArrayExpress. The clinical data associated with the GSE32894 and E-MTAB-1803 datasets contained the molecular subtype information for each sample.

Mutation and copy number alteration data. The mutation and copy number alteration data of TCGA samples were obtained from the supplementary file of the study reported by Robertson *et al* (3). The mutation data of E-MTAB-1803 and GSE48277 were obtained from the detailed sample information.

Data processing. Gene expression data, miRNA mature strand expression data, clinical data, mutation and copy number alteration data were integrated according to sample ID using Perl script. Values of GSE48277 dataset were \log_2 transformed by R script. The GSE32894, GSE48277 and E-MTAB-1803 datasets were further processed by R script. This included matching gene symbols, probes, calculating mean expression value for the gene symbol when several probes corresponded to one gene symbol, and defining mean value as the expression level of the gene symbol.

Immune infiltration analysis based on single-sample geneset enrichment analysis (ssGSEA) scores. To investigate the immune infiltration landscape of bladder cancer, ssGSEA was performed to assess the level of immune infiltration (recorded as ssGSEA score) in a sample according to the expression levels of immune cell-specific marker genes. Marker genes for most immune cell types were obtained from the article published by Bindea *et al* (16). Marker genes for M1 macrophages, M2 macrophages, myeloid-derived suppressor cells (MDSCs) and Tregs were obtained from published studies (10,14,17-25). The ssGSEA analysis was performed based on GenePattern environment (26). To run ssGSEA online analysis (<https://cloud.genepattern.org/>), gene expression dataset file (GCT file), immune marker gene set file (GMT file), and other parameters were uploaded as a set. Finally, the ssGSEA scores, representing infiltration levels of immune cells for individual samples, were presented in the output file.

Immune infiltration analysis based on cell type identification by estimating relative subsets of known RNA transcripts (CIBERSORT) method. The CIBERSORT analytical tool was developed to analyze the 22 distinct leukocyte subsets in the tumors based on bulk transcriptome data (27). CIBERSORT (<https://cibersort.stanford.edu/>) was employed to analyze the immune landscape of bladder cancer microenvironment based on the TCGA RNA-seq dataset. The TCGA RNA-seq dataset

was used as the gene expression input and LM22 (22 immune cell types) was set as the signature gene file. The analysis was conducted with 1,000 permutations. The CIBERSORT values generated were defined as immune cell infiltration fraction per sample.

RNA-seq analysis. A previous study from our group has used RNA-seq analysis of 10 tumor samples from patients with bladder cancer to identify novel prognostic biomarkers (28). These RNA-seq data were re-analyzed in the present study to investigate the TME, as aforementioned. Primary sequencing data (raw reads) were subjected to quality control and aligned to hg19 human genome. Reads per kilobase million (RPKM)-normalized values were computed to quantify gene expression levels. RNA-seq analysis and data processing was conducted by Beijing Genomics Institute (Shenzhen, China). Subsequently, the normalized data was analyzed by ssGSEA to quantify the immune infiltration levels in the tissue samples.

Immunohistochemical (IHC) assay. Formalin-fixed (10% formalin at room temperature for 24 h), paraffin-embedded tumor tissues were collected from 48 patients with bladder cancer (including the 10 patients enrolled in the aforementioned RNA sequencing analysis) diagnosed at Changhai Hospital, Shanghai, China, from December 2011 to June 2017. Written informed consent was obtained from all patients prior to surgery. The deparaffinized sections (4 μ m thickness) were incubated in Tris/EDTA buffer (pH 9.0) for antigen retrieval. Subsequently, blocking of endogenous peroxidase and non-specific epitopes were performed using the UltraSensitive IHC kit (cat. no. KIT-9710; Fuzhou Maixin Biotech.Co., Ltd.). The slides were incubated with primary antibodies at 4°C overnight, then with biotin-conjugated secondary antibodies at 37°C for 30 min and with streptavidin-peroxidase at room temperature for 10 min, using the UltraSensitive IHC kit. Immunostaining of slides was performed with 3,3'-diaminobenzidine followed by counterstaining with hematoxylin, dehydrating, and mounting. All mounted specimens were scanned into high resolution digital slides through slide scanners NanoZoomer-S60 (Hamamatsu Photonics). The primary antibodies were as follows: Monoclonal mouse anti-CD68 antibody (cat. no. M0876; 1:100 dilution; Dako; Agilent Technologies, Inc.), monoclonal rabbit anti-CD163 antibody (cat. no. ab182422; 1:500 dilution; Abcam) and monoclonal rabbit anti-CD31 antibody (cat. no. ab207090; 1:2,000 dilution; Abcam).

The IHC results for CD68 and CD163 were analyzed via a combination of the scores based on the percentage of positively stained cells (0, negative; 1, <15%; 2, 15-50%; 3, >50%) and the scores based on the color intensity (0, negative staining; 1+, weak staining, light yellow; 2+, moderate staining, yellow brown; and 3+, strong staining, brown). Samples with IHC score \leq 3 were defined as low expression, while samples with IHC score $>$ 3 were defined as high expression. Microvessels were evaluated by CD31 IHC staining, as described previously (29). Slides were first observed at x100 magnification to identify hotspots with the highest density of microvessels and each hotspot was then evaluated at x400 magnification. Any brown-staining endothelial cell or cell cluster was considered a countable microvessel.

Statistical analysis. For ssGSEA scores, CIBERSORT values, miRNA expression values and microvessel counts, comparison between two groups was conducted using the Mann-Whitney test for data with abnormal distribution and Student's t-test for data with normal distribution. Survival analyses were performed using Kaplan-Meier curves and log-rank test. IHC results (scores) for CD68 and CD163 were analyzed by Chi-square test. Pearson correlation analysis was used to estimate the consistency between ssGSEA scores and IHC scores in assessing M2 macrophage infiltration, and between miRNA expression values and ssGSEA scores of M2 macrophage. Statistical analysis was performed using SPSS pack 13.0 statistical software (SPSS, Chicago, IL, USA) and GraphPad Prism 7.0 software (GraphPad Software, Inc.). $P < 0.05$ was considered to indicate a statistically significant difference.

Results

Immune landscape related to histopathologic characteristics of bladder cancer. To explore the influence of immune cells on the malignant progression of bladder cancer, first, the RNA-seq data of 426 patients with bladder cancer from TCGA database were analyzed to evaluate the immune landscape. The marker genes of the majority of types of immune cells were evaluated between low and high histologic grade bladder cancer samples in TCGA dataset. The results revealed that B cells, macrophages and M2 macrophages were enriched in high grade bladder cancer, as presented in the corresponding heat map in Fig. 1A. Given that ssGSEA had previously been implemented to determine the immune landscape in clear cell renal cell carcinoma by utilizing RNA-seq data (7), the infiltration of each immune cell in the bladder cancer RNA-seq data was quantitatively analyzed using this method. The results indicated that B cells, macrophages, neutrophils, NK CD56dim cells, NK cells, T helper (Th) 1 cells, Th2 cells, MDSCs, Tregs and M2 macrophages were significantly enriched in high grade compared with low grade bladder cancer tissues (Fig. 1B). CIBERSORT was next applied to statistically estimate the relative proportions of immune cell subsets among different grades of bladder cancer samples in the TCGA dataset, following the method reported by Gentles *et al* (27). It was demonstrated that the infiltration levels of macrophage subsets (M0/M1/M2) and CD4 cell subsets (memory activated/memory resting) were higher in high grade bladder cancer. Furthermore, M2 macrophages accounted for the largest proportion among the 22 subsets of tumor-infiltrating immune cells, suggesting that they may have a key role in the progression of bladder cancer (Fig. 1C). Data from the GSE32894 dataset were used to validate the composition and proportion of tumor-infiltrating immune cell subsets in bladder cancer. The results were consistent with those observed in TCGA dataset, with higher levels of macrophage and M2 macrophage infiltration in the high-grade tumors compared with the low-grade tumors (Fig. 1D).

The immune cell infiltration in different pathologic stages of bladder cancer was then explored. As presented in Fig. 2A-C, in the TCGA dataset, B cells, macrophages and M2 macrophages exhibited a high infiltration level in higher compared

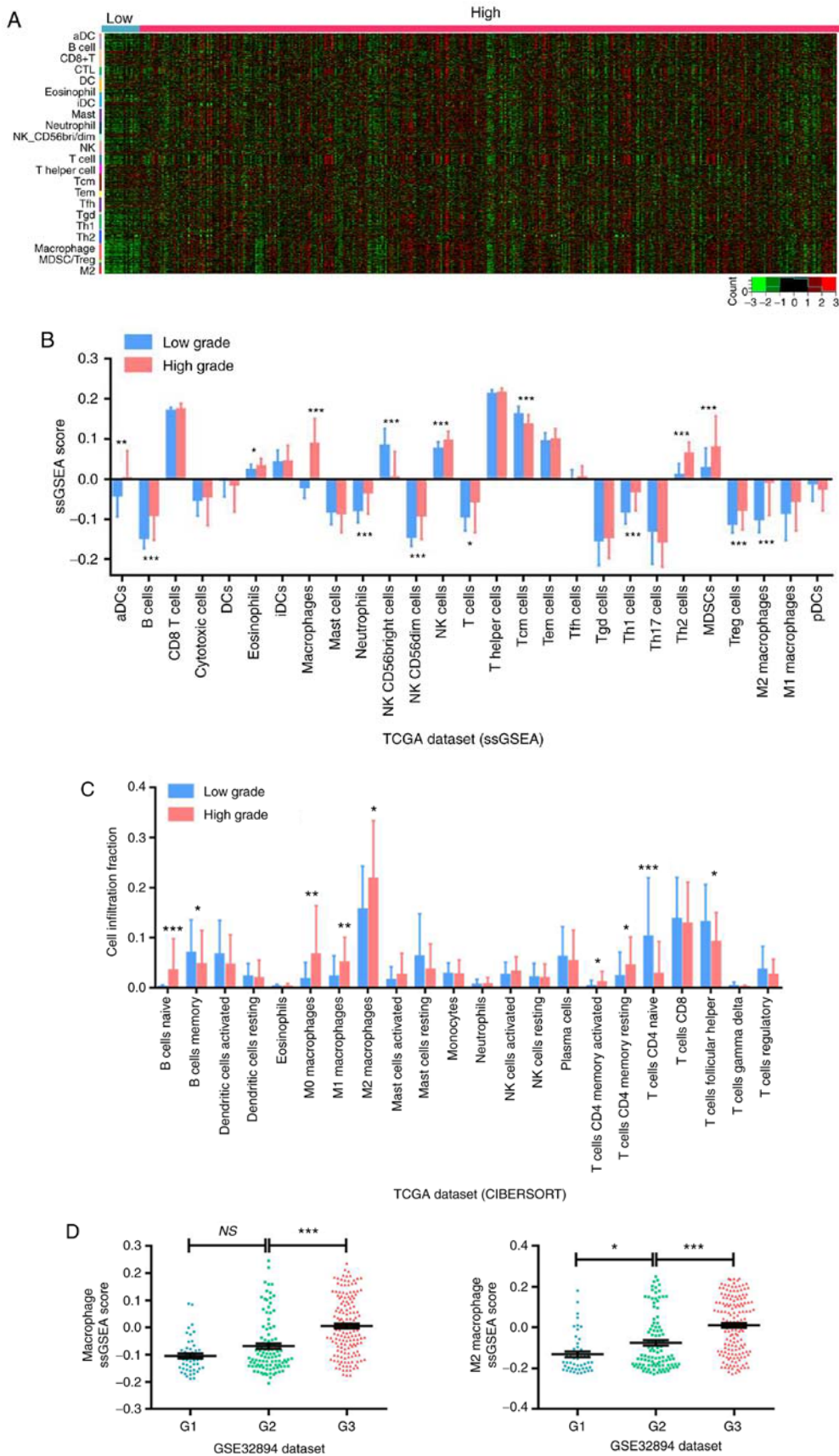


Figure 1. Analysis of immune landscape associated with bladder cancer histologic grade. (A) Heatmap showing the immune infiltration landscape between bladder cancer samples of different grades from TCGA database. Immune cell types were defined by specific gene markers. (B) Immune infiltration landscape analyzed by ssGSEA score-based method in bladder cancer samples from TCGA dataset. (C) Immune infiltration patterns analyzed by CIBERSORT method in bladder cancer samples with different grades from TCGA dataset. (D) Macrophage and M2 macrophage infiltration profiles assessed by ssGSEA in bladder cancer samples of different grades from the GSE32894 validation dataset. * $P < 0.05$, ** $P < 0.01$ and *** $P < 0.001$, with comparisons indicated by brackets. TCGA, The Cancer Genome Atlas; ssGSEA, single-sample genest enrichment analysis; CIBERSORT, Cell type Identification By Estimating Relative Subsets Of known RNA Transcripts; ns, not significant.

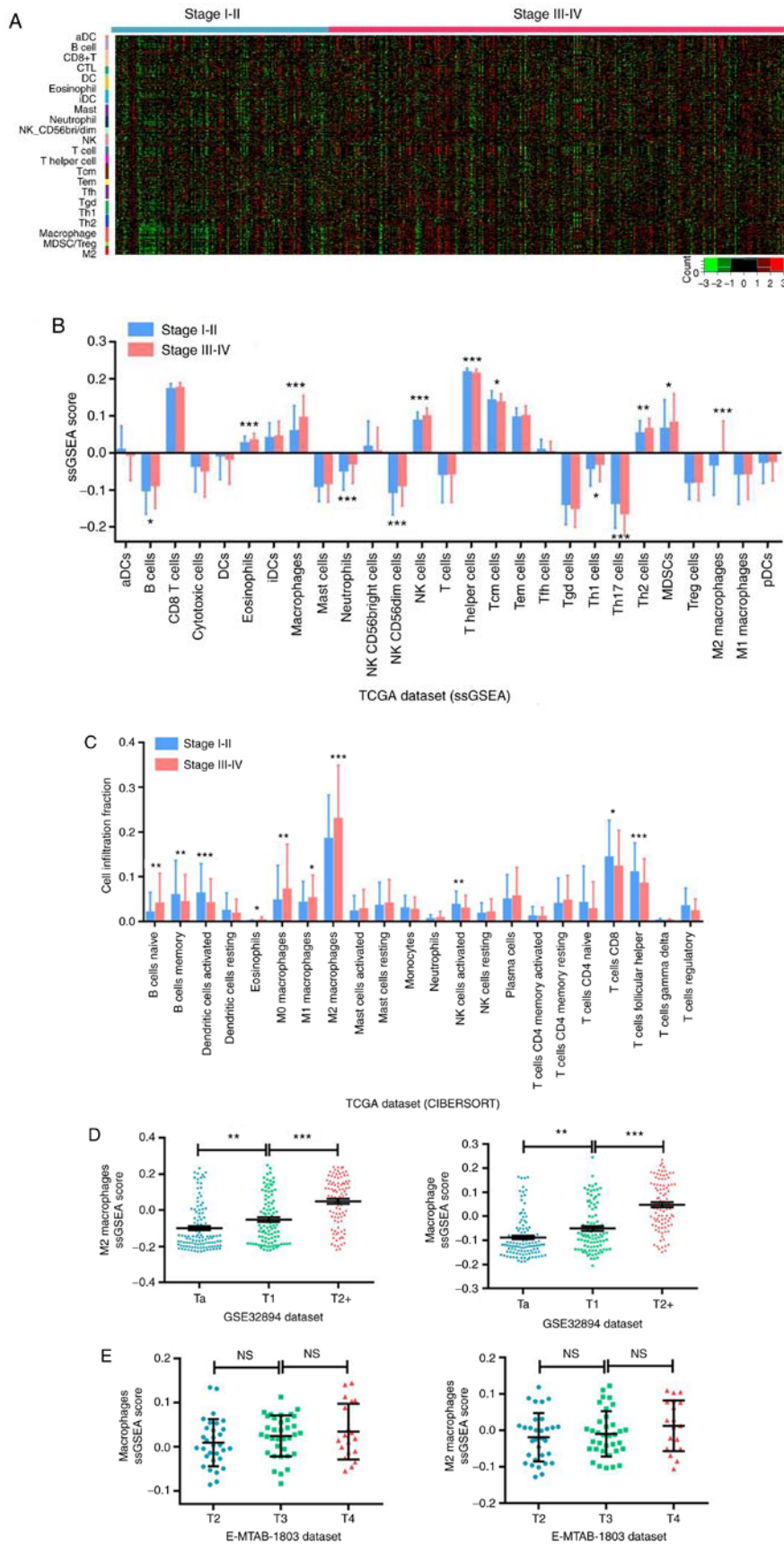


Figure 2. Immune infiltration profile in bladder cancer associated with pathologic stage. (A) Heatmap showing the immune infiltration patterns in bladder cancer samples with different stages from TCGA dataset. Immune cell types were defined by specific gene markers. (B) Immune infiltration patterns analyzed by ssGSEA score-based method in bladder cancer samples from TCGA dataset. (C) Immune infiltration patterns analyzed by CIBERSORT method in bladder cancer samples with different stages from TCGA dataset. (D, E) Macrophage and M2 macrophage infiltration profiles estimated by ssGSEA in bladder cancer samples with different stages from the GSE32894 and E-MTAB-1803 validation datasets. * $P < 0.05$, ** $P < 0.01$ and *** $P < 0.001$, with comparisons indicated by brackets. TCGA, The Cancer Genome Atlas; ssGSEA, single-sample geneset enrichment analysis; CIBERSORT, Cell type Identification By Estimating Relative Subsets Of known RNA Transcripts; ns, not significant.

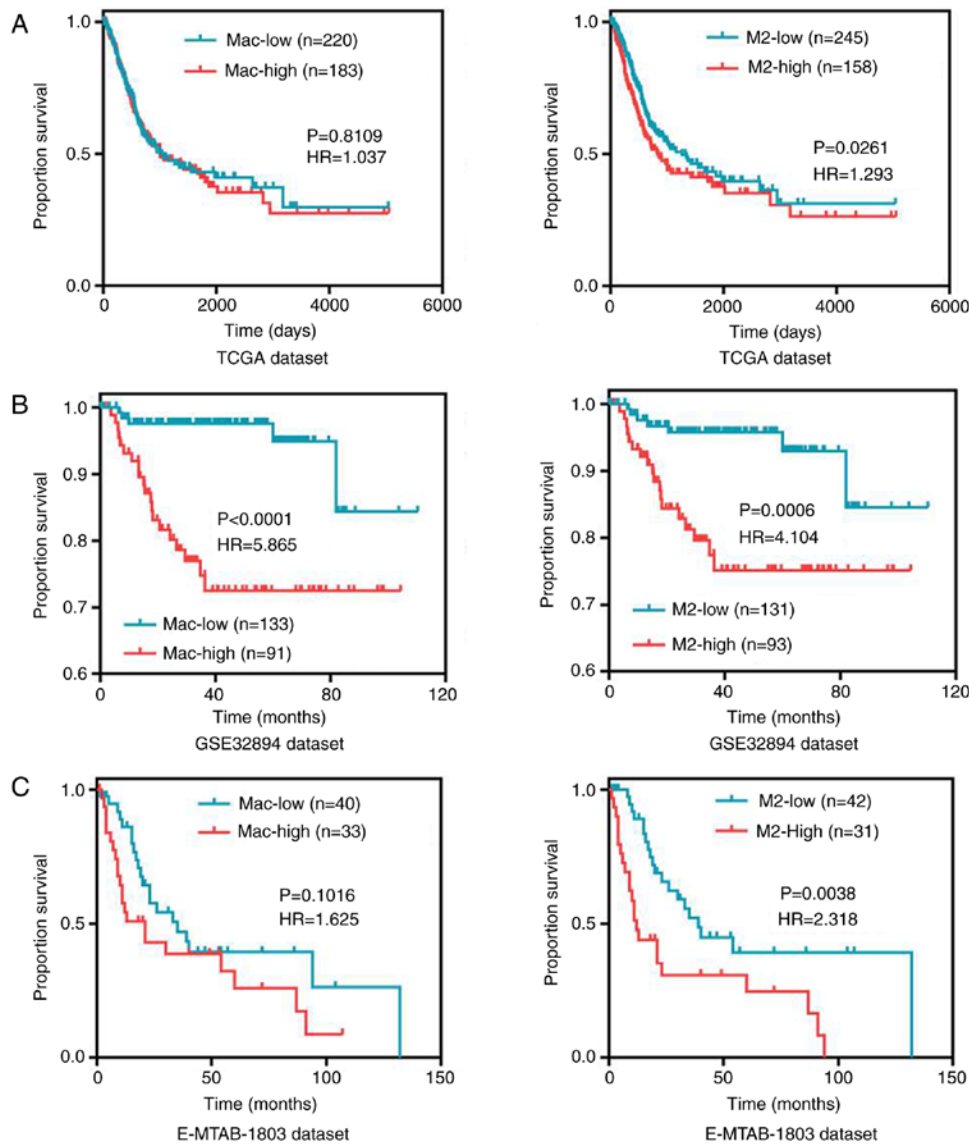


Figure 3. High M2 macrophage infiltration is associated with poor survival in bladder cancer patients. (A) Kaplan-Meier curves for overall survival in the high (above median) and low (below median) level groups for macrophage or M2 macrophage in bladder cancer based on TCGA dataset. (B) Disease-specific survival analysis between samples with different macrophage or M2 macrophage infiltration levels based on GSE32894 dataset. (C) Validation analysis of macrophage or M2 macrophage infiltration-related overall survival in E-MTAB-1803 dataset. TCGA, The Cancer Genome Atlas; Mac, macrophage.

with lower stage bladder cancer, with M2 macrophages having the highest proportion. Furthermore, the infiltration levels of macrophages and M2 macrophages were positively associated with the pathologic stage of bladder cancer, as confirmed by the data analysis from the validation datasets GSE32894 (Fig. 2D) and E-MTAB-1803 (Fig. 2E).

In summary, the present results demonstrated that the infiltration levels or proportions of macrophages, especially M2 macrophages, were positively associated with histologic grade and pathologic stage of bladder cancer, suggesting that M2 macrophages may be involved in the progression of bladder cancer.

Association of M2 macrophage infiltration with the prognosis of patients with bladder cancer. Kaplan-Meier survival curve analysis and ssGSEA scores were used to further explore the effect of M2 macrophage infiltration on the prognosis of patients with bladder cancer. In TCGA dataset, it was observed

that patients with high infiltration of M2 macrophages had worse overall survival compared with patients with low infiltration (Fig. 3A). No significant difference was observed in patient survival with varying total macrophage infiltration (Fig. 3A). Patients in the validation dataset GSE32894 with high macrophage and M2 macrophage infiltration exhibited worse disease-free survival (Fig. 3B). Finally, patients in the validation dataset E-MTAB-1803 with high M2 macrophage infiltration (but not total macrophage infiltration) exhibited worse overall survival (Fig. 3C). Consequently, high infiltration of M2 macrophages was associated with poor prognosis in patients with bladder cancer.

Validation of macrophage and M2 macrophage infiltration in bladder cancer. To confirm the infiltration of macrophages and M2 macrophages in tumor tissues from patients with bladder cancer in Eastern China, the present study calculated the immune infiltration scores for 10 newly collected tumor

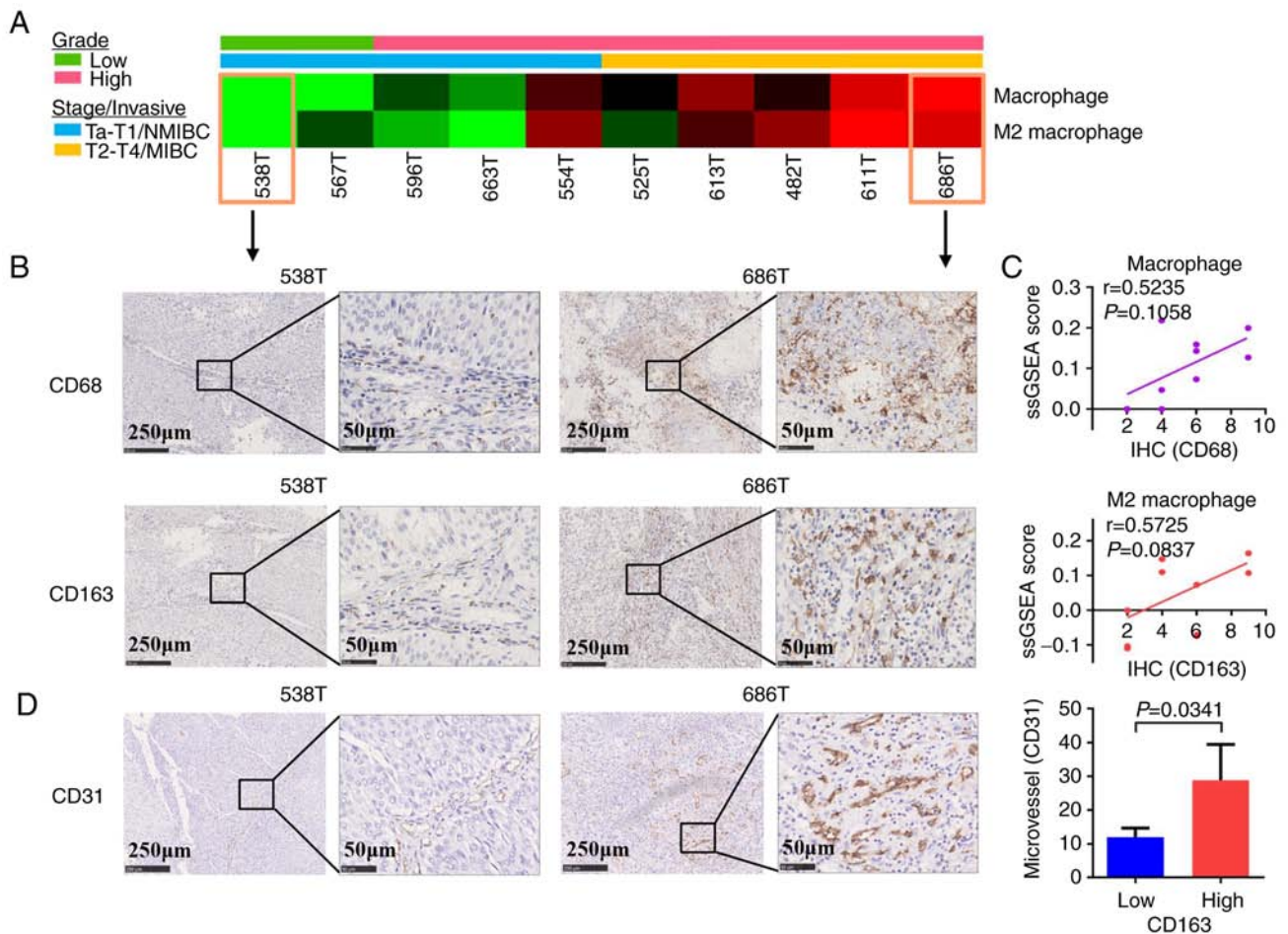


Figure 4. Validation analysis of macrophage and M2 macrophage infiltration in bladder cancer. (A) Heatmap showing macrophage and M2 macrophage infiltration profiles in 10 bladder cancer samples, based on ssGSEA score-computing RNA-seq gene expression. (B) IHC staining with CD68 and CD163 antibodies to determine macrophage and M2 macrophage infiltration, respectively, in two representative samples. (C) Correlation analysis comparing the consistency of the two methods (ssGSEA and IHC) for estimating macrophage and M2 macrophage infiltration levels. (D) IHC assay of microvessel density (staining for CD31) in a set of bladder cancer samples with different grades, stages and infiltrations of M2 macrophages. ssGSEA, single-sample genest enrichment analysis; RNA-seq, RNA sequencing; IHC, immunohistochemistry; NMIBC, non-muscle invasive bladder cancer; MIBC, muscle invasive bladder cancer.

tissues with different histologic grades and pathologic stages (NMIBC or MIBC) via analyzing RNA-seq data with ssGSEA algorithm. It was demonstrated that higher grade and stage (MIBC) bladder cancer tissues had higher infiltration levels of macrophages and M2 macrophages, compared with lower grade and stage (NMIBC) bladder cancer tissues (Fig. 4A). Consequently, the infiltration of macrophages and M2 macrophages in the 10 samples was evaluated by IHC staining with anti-CD68 and anti-CD163 antibody, respectively. IHC scores revealed that there was high macrophage and M2 macrophage infiltration in higher grade and stage bladder cancer tissues (MIBC) compared with lower grade and stage (NMIBC) bladder cancer tissues (Fig. 4B). In addition, the IHC scores were consistent with the ssGSEA scores in the same bladder cancer patient. Pearson correlation analysis was used to evaluate the consistency between the IHC scores and ssGSEA scores, and the results revealed that the two methods were positively correlated, albeit not significantly (Fig. 4C). The reason for the lack of statistical significance may be related to the small numbers of samples used. Further analysis of the infiltration of macrophages and M2 macrophages in 48 tumor tissues by IHC revealed that macrophages and M2 macrophages

were associated with the grade and the invasiveness/stage of bladder cancer, but not with age or sex (Table I). To investigate the relationship between tumor-infiltrating M2 macrophages and angiogenesis, IHC experiments were performed for the evaluation of microvessel density via staining of CD31 in the 10 samples. The results revealed that there were more microvessels in higher grade and stage bladder cancer tissues and that the microvessel count was significantly higher in the CD163-high compared with the CD163-low tissues (Fig. 4C).

M2 macrophage infiltration varies by molecular subtype in MIBC. Based on the high M2 macrophage infiltration in MIBC, further investigations were conducted on whether M2 macrophage infiltration was associated with the transcriptional molecular subtypes of MIBC. Analysis of the association of the RNA-seq data from TCGA database with the ssGSEA scores revealed that macrophages and M2 macrophages displayed significantly different infiltration levels among the MIBC subtypes (Fig. 5A), with the highest infiltration observed in the basal-squamous subtype, as defined by a previous study using TCGA dataset (30). This was consistent with the aforementioned results, where the infiltration of macrophages

Table I. Macrophage and M2 macrophage infiltration in bladder cancer samples as analyzed by immunohistochemistry staining.

Variable	CD68 expression			CD163 expression		
	High	Low	P-value	High	Low	P-value
Sex						
Male	21	14	0.740	20	15	0.522
Female	9	4		9	4	
Age (years)						
≥60	22	8	0.066	21	9	0.127
<60	8	10		8	10	
Grade						
Low-grade	6	12	0.002	5	13	0.001
High-grade	24	6		24	6	
Invasiveness						
NMIBC	10	10	0.019	9	11	0.008
MIBC	19	3		19	3	

NMIBC, non-muscle invasive bladder cancer; MIBC, muscle invasive bladder cancer.

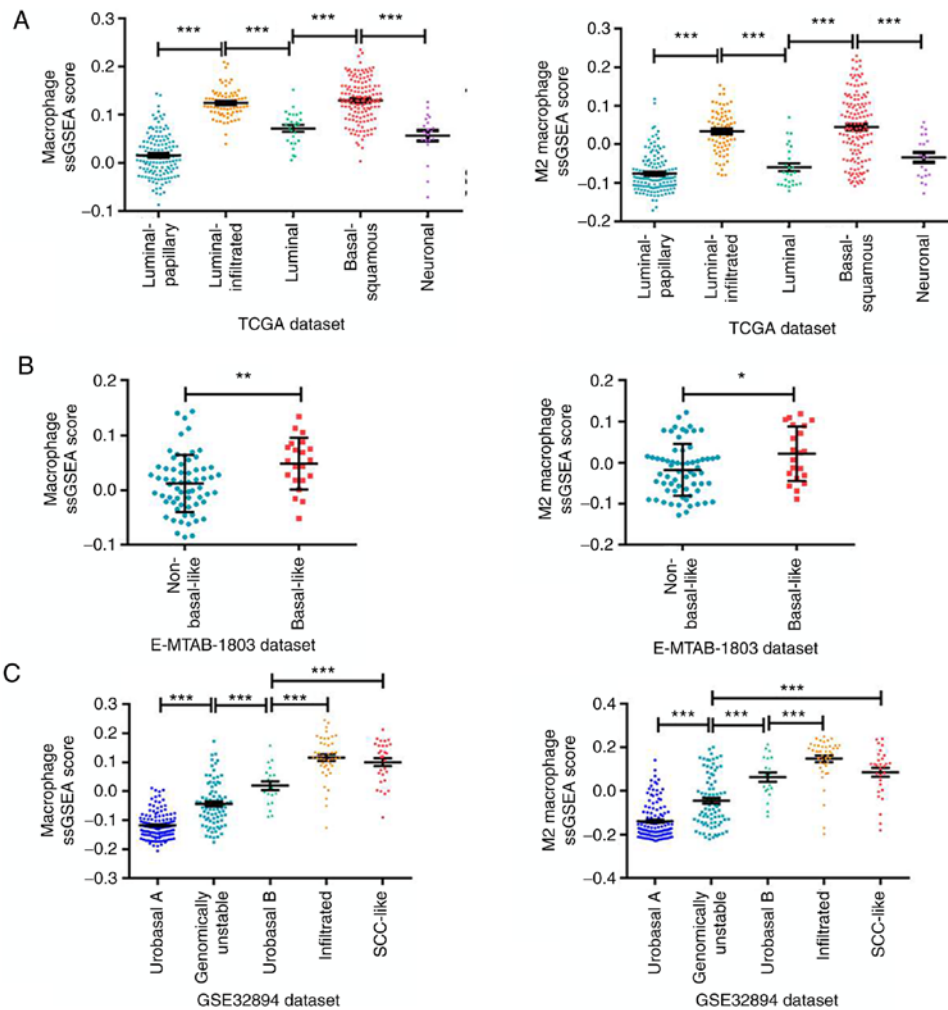


Figure 5. M2 macrophage infiltration varies by molecular subtype in MIBC. (A) Comparison of macrophage and M2 macrophage infiltration in MIBC samples with different molecular subtypes from TCGA dataset. (B) Validation analyses of macrophage and M2 macrophage infiltration profiles in MIBC samples with different molecular subtypes based on the E-MTAB-1803 and (C) GSE32894 datasets. The immune infiltration levels were estimated by the ssGSEA-score method. *P<0.05, **P<0.01 and ***P<0.001, with comparisons indicated by brackets. MIBC, muscle invasive bladder cancer; TCGA, The Cancer Genome Atlas; ssGSEA, single-sample genest enrichment analysis.

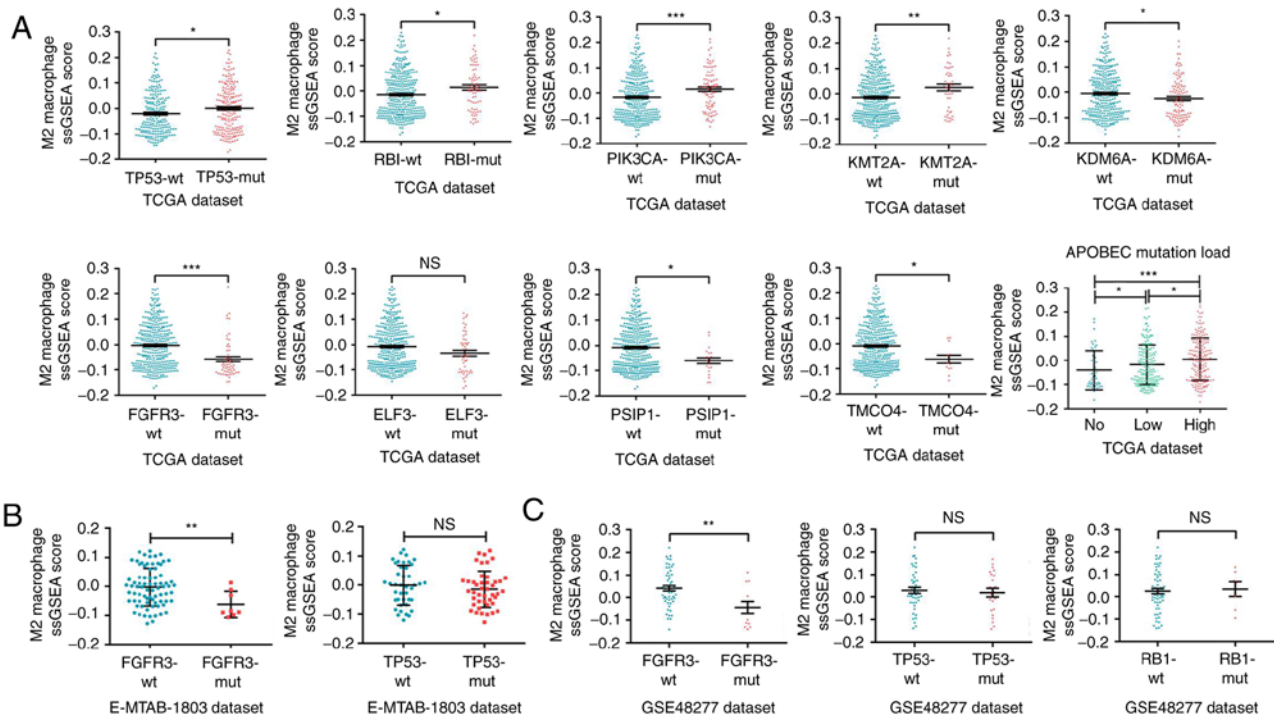


Figure 6. M2 macrophage infiltration is associated with specific mutations in bladder cancer. (A) Analyses of M2 macrophage infiltration profiles in bladder cancer samples with various mutant statuses from TCGA dataset. (B) Validation analyses of M2 macrophage infiltration profiles in samples with FCFR3 and TP53 mutant statuses from the E-MTAB-1803 and (C) GSE48277 datasets. * $P < 0.05$, ** $P < 0.01$ and *** $P < 0.001$, with comparisons indicated by brackets. TCGA, The Cancer Genome Atlas; RB1, RB transcriptional corepressor 1; PIK3CA, phosphatidylinositol-4,5-bisphosphate 3-kinase catalytic subunit α ; KMT2A, lysine methyltransferase 2A; KDM6A, lysine demethylase 6A; FGFR3, growth factor receptor 3; ELF3, E74-like ETS transcription factor 3; PSIP1, PC4 and SFRS1 interacting protein 1; TMCO4, transmembrane and coiled-coil domains 4; APOBEC, apolipoprotein B mRNA editing enzyme catalytic-polypeptide-like; ns, not significant.

and M2 macrophages was higher in bladder cancer with higher grade and stage and associated with low survival and poor prognosis of patients with basal-squamous subtype. In addition, macrophage and M2 macrophage infiltration was significantly higher in the basal-like subtype in the validation dataset E-MTAB-1803 (Fig. 5B), similar to the basal-squamous subtype in TCGA classification. Finally, it was confirmed in the validation dataset GSE32894 that macrophage and M2 macrophage infiltration was higher in the infiltrated and SCC-like subtypes (5,31), which are similar to the basal subtype. These results indicated that the macrophage and M2 macrophage infiltration was associated with molecular subtypes of MIBC. Additionally, M2 macrophages accounted for the majority proportion of all subtypes of infiltrating macrophages in bladder cancer, as presented in Figs. 1C and 2C, which indicated that the infiltration of M2 macrophages may provide a good estimate of the overall macrophage population in bladder cancer.

M2 macrophage infiltration is associated with specific mutations in bladder cancer. The discovery that the infiltration of macrophages, especially M2 macrophages, was associated with malignant progression of bladder cancer and with the molecular subtypes of MIBC implied that specific intrinsic genomics might affect the infiltration of M2 macrophages. Therefore, the difference in M2 macrophage infiltration levels among different gene mutation types was explored. Analysis of a large number of mutant genes using ssGSEA algorithm in the TCGA dataset revealed that the M2 macrophage infiltration levels differed among multiple mutant genes. As presented in Fig. 6A,

the M2 macrophage infiltration was higher in bladder tumor tissues with mutant TP53, RB transcriptional corepressor 1 (RB1), phosphatidylinositol-4,5-bisphosphate 3-kinase catalytic subunit α (PIK3CA), lysine methyltransferase 2A (KMT2A), lysine demethylase 6A (KDM6A) and apolipoprotein B mRNA editing enzyme catalytic-polypeptide-like (APOBEC), but lower in tissues with mutant fibroblast growth factor receptor 3 (FGFR3), E74-like ETS transcription factor 3 (ELF3), PC4 and SFRS1 interacting protein 1 (PSIP1) and transmembrane and coiled-coil domains 4 (TMCO4). In the validation datasets E-MTAB-1803 and GSE48277, it was confirmed that M2 macrophage infiltration was lower in tissues with mutant FGFR3 (Fig. 6B and C); however, no significant difference was observed for the mutation status of TP53 and RB1 (Fig. 6B and C). In summary, M2 macrophage infiltration varied among bladder cancer mutant gene types, suggesting that specific mutations may influence M2 macrophage infiltration.

M2 macrophage infiltration is correlated with specific copy number variations in bladder cancer. Further exploration was performed on whether there were differences in the M2 macrophage infiltration among different bladder cancer-specific copy number variations. It was demonstrated that the M2 macrophage infiltration was influenced by specific amplification types of copy number variations. The results of the ssGSEA algorithm in TCGA dataset indicated that the infiltration in the tissues with amplified FGFR3, erb-b2 receptor tyrosine kinase 2 (ERBB2), BCL2-like 1 (BCL2L1), telomerase reverse transcriptase (TERT)

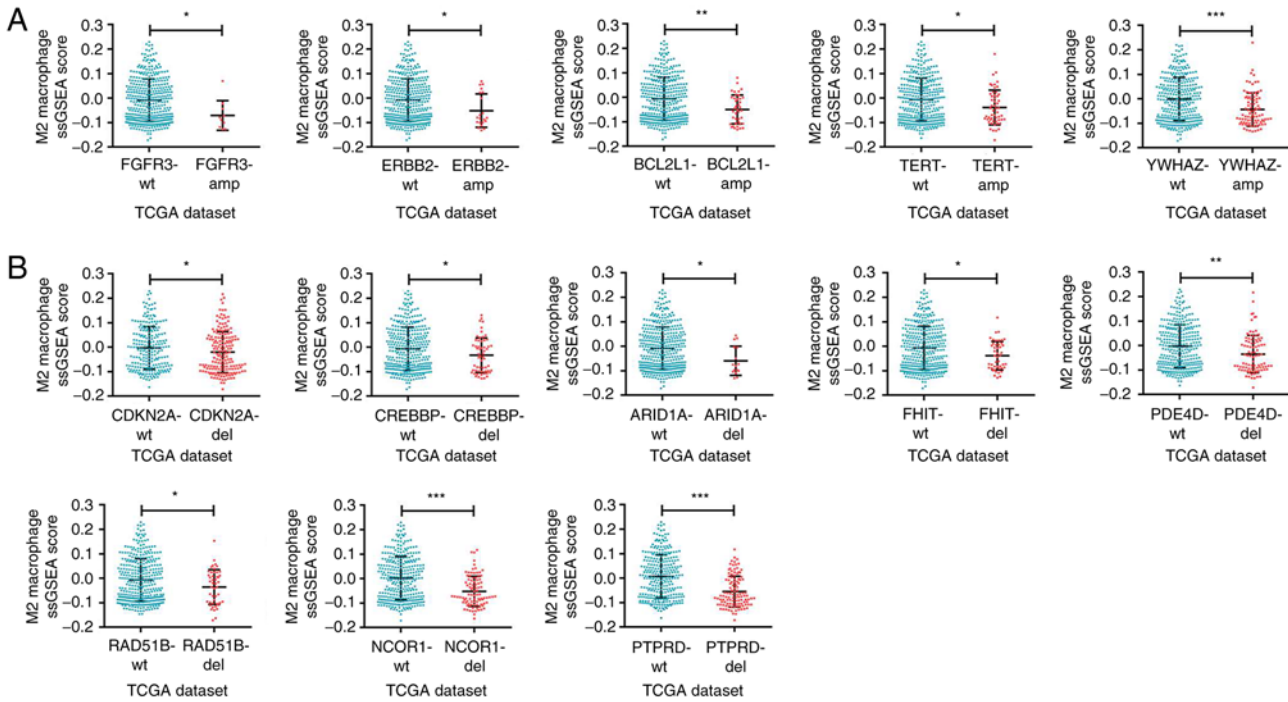


Figure 7. M2 macrophage infiltration is associated with specific copy number alterations in bladder cancer. (A) Analyses of M2 macrophage infiltration profiles in bladder cancer samples with specific amplification of gene copy number from TCGA dataset. (B) M2 macrophage infiltration profiles in bladder cancer samples with specific deletion of gene copy number from TCGA dataset. * $P < 0.05$, ** $P < 0.01$ and *** $P < 0.001$, with comparisons indicated by brackets. TCGA, The Cancer Genome Atlas; FGFR3, growth factor receptor 3; ERBB2, erb-b2 receptor tyrosine kinase 2; BCL2L1, BCL2-like 1; TERT, telomerase reverse transcriptase; YWHAZ, tyrosine-3-monooxygenase/tryptophan-5-monooxygenase activation protein ζ ; CDKN2A, cyclin-dependent kinase inhibitor 2A; CREBBP, CREB binding protein; ARID1A, AT-rich interaction domain 1A; FHIT, fragile histidine triad diadenosine triphosphatase; PDE4D, phosphodiesterase 4D; RAD51B, RAD51 paralog B; NCOR1, nuclear receptor corepressor 1; PTPRD, protein tyrosine phosphatase receptor type D.

and tyrosine-3-monooxygenase/tryptophan-5-monooxygenase activation protein ζ (YWHAZ) and with deleted cyclin-dependent kinase inhibitor 2A (CDKN2A), CREB binding protein (CREBBP), AT-rich interaction domain 1A (ARID1A), fragile histidine triad diadenosine triphosphatase (FHIT), phosphodiesterase 4D (PDE4D), RAD51 paralog B (RAD51B), nuclear receptor corepressor 1 (NCOR1) and protein tyrosine phosphatase receptor type D (PTPRD) was significantly reduced (Fig. 7A and B, respectively). Thus, the intrinsic specific copy number variations of bladder cancer and related molecular mechanisms may influence the M2 macrophage infiltration in the TME of bladder cancer.

M2 macrophage infiltration is associated with differentially expressed miRNAs in bladder cancer. To further investigate the mechanisms of modulating the tumor-infiltrating M2 macrophages in bladder cancer, miRNA expression data were analyzed between tissues containing wild type and mutant TP53, RB1, PIK3CA, KMT2A, KDM6A, FGFR3, ELF3, PSIP1, TMCO4, and APOBEC. There was not a specific miRNA consistently expressed differentially in all of the mutant genes. Since the PIK3CA mutation has been previously reported to be associated with macrophage infiltration (32), miRNAs expressed differentially ($P < 0.1$) between wild type and mutant type of PIK3CA were selected. The differential expression of these miRNAs in the remaining mutant genes were analyzed in sequence. Seven miRNAs (miR-214-5p, miR-223-3p, miR-155-5p, miR-199a-3p, miR-199b-3p, miR-146b-5p, miR-142-5p),

which were expressed differentially in at least three mutant genes and positively correlated with M2 macrophage infiltration, as well as expressed highly in high grade bladder cancer, were finally identified (Fig. 8A-C). The differential expression of these miRNAs in each copy number variant subtype and stage of bladder cancer was further analyzed (Fig. S1).

Discussion

The present study demonstrated that M2 macrophages were the predominant tumor-infiltrating immune cells in the bladder cancer microenvironment, most abundant in the 'basal' subtype of MIBC and associated with the histopathologic grade and stage, as well as the prognosis of patients. Furthermore, miRNAs expressed differentially due to cancer-specific genomic alterations were identified as potential triggers of M2 macrophage recruitment in the TME of bladder cancer.

Previous studies on the immune microenvironment of bladder cancer focused on a few selected immune cells, such as tumor-infiltrating dendritic cells (TIDCs), tumor-infiltrating lymphocytes (TILs), and TAMs (detected by immunohistochemical staining for CD68), and mostly involving a small number of samples (14,33-35). In the present study, ssGSEA and CIBERSORT algorithms were employed to explore the infiltration of various immune cells in a large-scale data and the results revealed that M2 macrophages were the main immune components in bladder cancer and were associated

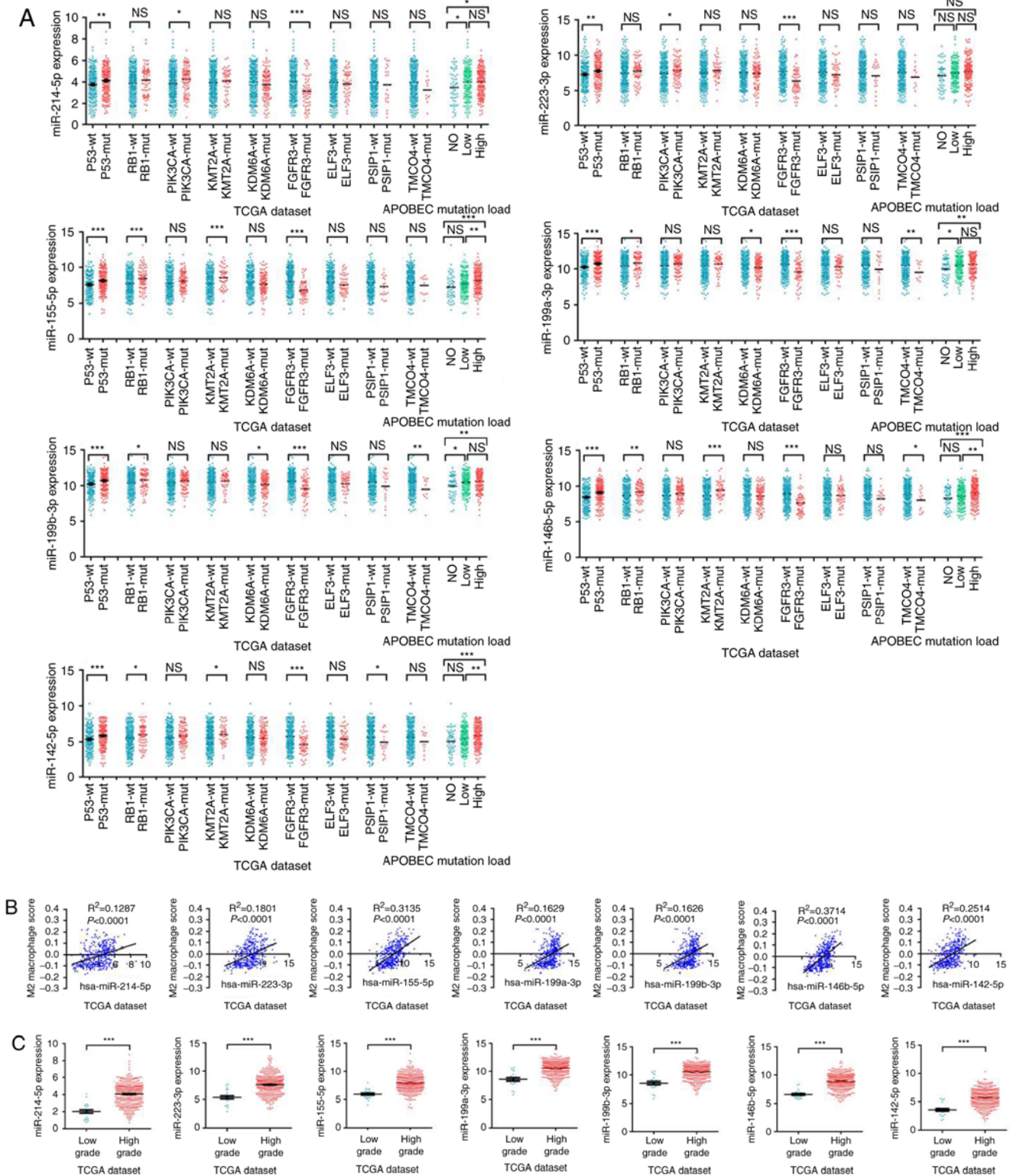


Figure 8. M2 macrophage infiltration is associated with differentially expressed miRNAs in bladder cancer. (A) Analyses of miRNA expression in bladder cancer samples with specific mutant status form TCGA dataset. (B) Correlation analyses between M2 macrophage infiltration and miRNA expression. (C) Analyses of miRNA expression in bladder cancer samples with different grades from TCGA dataset. * $P < 0.05$, ** $P < 0.01$ and *** $P < 0.001$, with comparisons indicated by brackets. miRNA, microRNA; TCGA, The Cancer Genome Atlas; ns, not significant.

with the progression of tumors and the poor prognosis of patients.

Numerous studies have investigated the bladder cancer-associated macrophages, focusing on the role of macrophages in the treatment of bladder cancer with Bacillus Calmette-Guerin

(BCG), neoadjuvant chemotherapy and immunological checkpoint inhibitors (15,35-37). However, few studies have focused on M2 macrophages. In the present study, high-throughput data obtained from multiple datasets were used to demonstrate the importance of M2 macrophages in bladder cancer progression.

Sjödahl *et al.* (14) observed that a high CD68/CD3 ratio reflected a poor prognosis among MIBC. Recently, Wu *et al.* (38) performed a meta-analysis and demonstrated that TAMs identified with CD68 alone were not significantly correlated with the prognosis of bladder cancer patients, but TAMs detected with CD163 were significantly correlated with poor relapse-free survival. Maniecki *et al.* (39) reported that CD163 mRNA expression in bladder cancer biopsies was associated with advanced tumor stages, aggressive tumor grade and poor overall survival. In addition, high tumor macrophage infiltration (by CD163-positive staining in IHC) was associated with advanced stage and tumor grade (39). Aljabery *et al.* (40) assessed bladder cancer samples from cystectomy by IHC and observed that M2 infiltration was not correlated to stage or grade, but appeared to be inversely correlated with improved cancer-specific survival; however, patients collected in their study were all MIBC and patients with NMIBC, which account for ~75% of all bladder cancer, were not included. In the present study, NMIBC and MIBC samples were included and analyzed, and M2 macrophages were demonstrated to be associated with histologic grade and pathologic stage of bladder cancer, as well as prognosis of patients with bladder cancer, based on large-scale data bioinformatics analysis and biological experimental analyses (IHC for CD163). These results suggested that M2 macrophages may be potential targets for immunotherapy of bladder cancer. The increased infiltration of TAMs (M2-like) is associated with a poor response to BCG in patients with NMIBC (35). The stromal immunotypes could effectively predict response to adjuvant chemotherapy, recurrence and survival in patients with MIBC (41). Nowadays, several approaches (including depletion of TAMs, inhibition of monocyte recruitment into the cancer, blockade of M2 macrophages, reprogramming of TAMs toward M1 macrophages) have been evaluated as strategies to target TAMs in cancer (42). Novel immunotherapies targeting M2 macrophages or their combination with immune checkpoint inhibitors may present promising results in the treatment of bladder cancer and other types of cancer (43,44).

In the present study, it was observed that microvessel count was significantly higher in bladder cancer tissues with highly infiltrated M2 macrophages, which indicated that M2 macrophages may stimulate angiogenesis (45). In addition, there were more microvessels in higher grade and stage bladder cancer tissues, which was consistent with the hypothesis that M2 macrophages promote neovascularization and cancer progression (46).

Tumor intrinsic genomics were found to affect the composition of the immune microenvironment. Molecular subtypes of glioblastoma differentially activate the immune microenvironment and the tumor-promoting M2 macrophages exhibit a high association with the mesenchymal subtype relative to proneural and classical subtypes (47). It has also been reported that TILs are associated with neurofibromin 1 and RB1 mutations, as well as epidermal growth factor receptor-amplified and homozygous PTEN-deleted alterations in glioblastomas (48). In the present study, the levels of M2 macrophage infiltration varied among different bladder cancer molecular subtypes, with the 'basal' subtype of MIBC having the highest infiltration levels. Several gene mutations and copy number variations were associated in the current study with M2 macrophage infiltration in bladder cancer. Bladder cancer cells can produce factors, such as

macrophage-colony stimulating factor or monocyte chemoattractant protein family-1, that trigger the amplification and mobilization of macrophages in the TME (49-51). Bladder cancer also affects macrophages by releasing and delivering miRNAs, which may impede the M1 phenotype polarization, drive M2 phenotype polarization of macrophages, or switch phenotypes from M1 to M2 by binding to downstream targets or macrophages (9,52,53). The current results demonstrated that there were miRNAs expressed differentially in cancer-specific genomic alterations, related with M2 macrophage infiltration, and highly expressed in high grade and advanced stage of bladder cancer. Taken together, these results indicated that the bladder cancer-specific genomic alterations may lead to differentially expressed miRNAs, that may subsequently influence M2 macrophage infiltration and promote bladder cancer progression. It has been suggested that exosomes mediate the communication between tumor cells and macrophages (54,55). Exosomes are a type of nanometric membrane vesicles released by cells into the extracellular environment, that regulate the biological activities of target cells via delivering DNAs, RNAs and proteins (56). Consequently, it can be speculated that bladder cancer with special genomic alterations may promote the recruitment and polarization of M2 macrophages in the TME via exosomal miRNAs. Future studies are required to validate this hypothesis and to explore the intrinsic genomic mechanisms affecting M2 macrophage infiltration, with the aim to provide a potential therapeutic target of immunotherapy for bladder cancer.

In conclusion, the present study demonstrated that M2 macrophages were the predominant tumor-infiltrating immune cells in bladder cancer. Their infiltration was associated with the histologic grade, pathologic stage of bladder cancer and 'basal' subtype of MIBC, as well as prognosis of patients. Differentially expressed miRNAs, associated with cancer-specific genomic alterations, may be important drivers of M2 macrophage infiltration, which may serve as a potential immunotherapy target for bladder cancer.

Acknowledgements

Not applicable.

Funding

The present study was supported by the National Natural Science Fund of China (grant no. 8150101083, 81572509), the Innovation Program of Shanghai Municipal Education Commission (grant no. 2017-01-07-00-07-E00014), the Leading Talents Training Program of Shanghai in 2017.

Availability of data and materials

The datasets used and/or analyzed during the current study are available from the corresponding author on reasonable request.

Authors' contributions

YX and LT conceived the study, performed the experiment, and wrote the manuscript. FL collected the clinical samples and data and participated in the analysis. AL, SZ, XH and

QX participated in the experiments. LT and ZY analyzed the data. CX and YS contributed to the initial design of the study, supervised the bioinformatic and experimental analyses, and critically edited the manuscript. All authors discussed the results and approved the final manuscript.

Ethics approval and consent to participate

The present study's protocol involving human subjects was approved by the Ethics Committee of Changhai Hospital of the Second Military Medical University (Shanghai, China). Written informed consent for using tumor tissue in scientific research was obtained from all patients.

Patient consent for publication

Not applicable.

Competing interests

The authors declare that they have no competing interests.

References

- Sanli O, Dobruch J, Knowles MA, Burger M, Alemozaffar M, Nielsen ME and Lotan Y: Bladder cancer. *Nat Rev Dis Primers* 3: 17022, 2017.
- Babjuk M, Böhle A, Burger M, Capoun O, Cohen D, Compérat EM, Hernández V, Kaasinen E, Palou J, Rouprêt M, *et al*: EAU guidelines on non-muscle-invasive urothelial carcinoma of the bladder: Update 2016. *Eur Urol* 71: 447-461, 2017.
- Robertson AG, Kim J, Al-Ahmadie H, Bellmunt J, Guo G, Cherniack AD, Hinoue T, Laird PW, Hoadley KA, Akbani R, *et al*: Comprehensive molecular characterization of muscle-invasive bladder cancer. *Cell* 171: 540-556.e25, 2017.
- Sjödahl G, Lauss M, Lövgren K, Chebil G, Gudjonsson S, Veerla S, Patschan O, Aine M, Fernö M, Ringnér M, *et al*: A molecular taxonomy for urothelial carcinoma. *Clin Cancer Res* 18: 3377-3386, 2012.
- Choi W, Porten S, Kim S, Willis D, Plimack ER, Hoffman-Censits J, Roth B, Cheng T, Tran M, Lee IL, *et al*: Identification of distinct basal and luminal subtypes of muscle-invasive bladder cancer with different sensitivities to frontline chemotherapy. *Cancer Cell* 25: 152-165, 2014.
- Zhang H, Ye YL, Li MX, Ye SB, Huang WR, Cai TT, He J, Peng JY, Duan TH, Cui J, *et al*: CXCL2/MIF-CXCR2 signaling promotes the recruitment of myeloid-derived suppressor cells and is correlated with prognosis in bladder cancer. *Oncogene* 36: 2095-2104, 2017.
- Kitamura T, Qian BZ and Pollard JW: Immune cell promotion of metastasis. *Nat Rev Immunol* 15: 73-86, 2015.
- Şenbabaoglu Y, Gejman RS, Winer AG, Liu M, Van Allen EM, de Velasco G, Miao D, Ostrovskaya I, Drill E, Luna A, *et al*: Tumor immune microenvironment characterization in clear cell renal cell carcinoma identifies prognostic and immunotherapeutically relevant messenger RNA signatures. *Genome Biol* 17: 231, 2016.
- Wang N, Liang H and Zen K: Molecular mechanisms that influence the macrophage m1-m2 polarization balance. *Front Immunol* 5: 614, 2014.
- Qian BZ and Pollard JW: Macrophage diversity enhances tumor progression and metastasis. *Cell* 141: 39-51, 2010.
- Na YR, Yoon YN, Son DI and Seok SH: Cyclooxygenase-2 inhibition blocks M2 macrophage differentiation and suppresses metastasis in murine breast cancer model. *PLoS One* 8: e63451, 2013.
- Ruffell B and Coussens LM: Macrophages and therapeutic resistance in cancer. *Cancer Cell* 27: 462-472, 2015.
- Korpala M, Puyang X, Jeremy Wu Z, Seiler R, Furman C, Oo HZ, Seiler M, Irwin S, Subramanian V, Julie Joshi J, *et al*: Evasion of immunosurveillance by genomic alterations of PPAR γ /RXR α in bladder cancer. *Nat Commun* 8: 103, 2017.
- Sjödahl G, Lövgren K, Lauss M, Chebil G, Patschan O, Gudjonsson S, Månsson W, Fernö M, Leandersson K, Lindgren D, *et al*: Infiltration of CD3 $^{+}$ and CD68 $^{+}$ cells in bladder cancer is subtype specific and affects the outcome of patients with muscle-invasive tumors. *Urol Oncol* 32: 791-797, 2014.
- Miyake M, Tatsumi Y, Gotoh D, Ohnishi S, Owari T, Iida K, Ohnishi K, Hori S, Morizawa Y, Itami Y, *et al*: Regulatory T cells and tumor-associated macrophages in the tumor microenvironment in non-muscle invasive bladder cancer treated with intravesical Bacille Calmette-Guérin: A long-term follow-up study of a Japanese Cohort. *Int J Mol Sci* 18: pii: E2186, 2017.
- Bindea G, Mlecnik B, Tosolini M, Kirilovsky A, Waldner M, Obenauf AC, Angell H, Fredriksen T, Lafontaine L, Berger A, *et al*: Spatiotemporal dynamics of intratumoral immune cells reveal the immune landscape in human cancer. *Immunity* 39: 782-795, 2013.
- Sanyal R, Polyak MJ, Zuccolo J, Puri M, Deng L, Roberts L, Zuba A, Storek J, Luider JM, Sundberg EM, *et al*: MS4A4A: A novel cell surface marker for M2 macrophages and plasma cells. *Immunol Cell Biol* 95: 611-619, 2017.
- Ambarus CA, Krausz S, van Eijk M, Hamann J, Radstake TR, Reedquist KA, Tak PP and Baeten DL: Systematic validation of specific phenotypic markers for in vitro polarized human macrophages. *J Immunol Methods* 375: 196-206, 2012.
- Lugo-Villarino G, Troegeler A, Balboa L, Lastrucci C, Duval C, Mercier I, Bénard A, Capilla F, Al Saati T, Poincloux R, *et al*: The C-type lectin receptor DC-SIGN has an anti-inflammatory role in human M(IL-4) macrophages in response to *Mycobacterium tuberculosis*. *Front Immunol* 9: 1123, 2018.
- Choi JW, Kwon MJ, Kim IH, Kim YM, Lee MK and Nam TJ: Pyropia yezoensis glycoprotein promotes the M1 to M2 macrophage phenotypic switch via the STAT3 and STAT6 transcription factors. *Int J Mol Med* 38: 666-674, 2016.
- Liu M, Yang W, Liu S, Hock D, Zhang B, Huo RY, Tong X and Yan H: LXRA is expressed at higher levels in healthy people compared to atherosclerosis patients and its over-expression polarizes macrophages towards an anti-inflammatory M Φ 2 phenotype. *Clin Exp Hypertens* 40: 213-217, 2018.
- Lo TH, Silveira PA, Fromm PD, Verma ND, Vu PA, Kupresanin F, Adam R, Kato M, Cogger VC, Clark GJ and Hart DN: Characterization of the expression and function of the C-type lectin receptor CD302 in mice and humans reveals a role in dendritic cell migration. *J Immunol* 197: 885-898, 2016.
- Bellora F, Castriconi R, Dundero A, Reggiardo G, Moretta L, Mantovani A, Moretta A and Bottino C: The interaction of human natural killer cells with either unpolarized or polarized macrophages results in different functional outcomes. *Proc Natl Acad Sci USA* 107: 21659-21664, 2010.
- Ornstein MC, Diaz-Montero CM, Rayman P, Elson P, Haywood S, Finke JH, Kim JS, Pavicic PG Jr, Lamenza M, Devonshire S, *et al*: Myeloid-derived suppressor cells (MDSC) correlate with clinicopathologic factors and pathologic complete response (pCR) in patients with urothelial carcinoma (UC) undergoing cystectomy. *Urol Oncol* 36: 405-412, 2018.
- Gielen PR, Schulte BM, Kers-Rebel ED, Verrijp K, Petersen-Baltussen HM, ter Laan M, Wesseling P and Adema GJ: Increase in both CD14-positive and CD15-positive myeloid-derived suppressor cell subpopulations in the blood of patients with glioma but predominance of CD15-positive myeloid-derived suppressor cells in glioma tissue. *J Neuropathol Exp Neurol* 74: 390-400, 2015.
- Reich M, Liefeld T, Gould J, Lerner J, Tamayo P and Mesirov JP: GenePattern 2.0. *Nat Genet* 38: 500-501, 2006.
- Gentles AJ, Newman AM, Liu CL, Bratman SV, Feng W, Kim D, Nair VS, Xu Y, Khuong A, Hoang CD, *et al*: The prognostic landscape of genes and infiltrating immune cells across human cancers. *Nat Med* 21: 938-945, 2015.
- Zeng S, Yu X, Ma C, Song R, Zhang Z, Zi X, Chen X, Wang Y, Yu Y, Zhao J, *et al*: Transcriptome sequencing identifies ANLN as a promising prognostic biomarker in bladder urothelial carcinoma. *Sci Rep* 7: 3151, 2017.
- Chai CY, Chen WT, Hung WC, Kang WY, Huang YC, Su YC and Yang CH: Hypoxia-inducible factor-1 α expression correlates with focal macrophage infiltration, angiogenesis and unfavourable prognosis in urothelial carcinoma. *J Clin Pathol* 61: 658-664, 2008.
- Cancer Genome Atlas Research Network: Comprehensive molecular characterization of urothelial bladder carcinoma. *Nature* 507: 315-322, 2014.

31. Perou CM, Sørliie T, Eisen MB, van de Rijn M, Jeffrey SS, Rees CA, Pollack JR, Ross DT, Johnsen H, Akslen LA, *et al*: Molecular portraits of human breast tumours. *Nature* 406: 747-752, 2000.
32. An Y, Adams JR, Hollern DP, Zhao A, Chang SG, Gams MS, Chung PED, He X, Jangra R, Shah JS, *et al*: Cdh1 and Pik3ca mutations cooperate to induce immune-related invasive lobular carcinoma of the breast. *Cell Rep* 25: 702-714.e6, 2018.
33. Hanada T, Nakagawa M, Emoto A, Nomura T, Nasu N and Nomura Y: Prognostic value of tumor-associated macrophage count in human bladder cancer. *Int J Urol* 7: 263-269, 2000.
34. Ayari C, LaRue H, Hovington H, Decobert M, Harel F, Bergeron A, Têtu B, Lacombe L and Fradet Y: Bladder tumor infiltrating mature dendritic cells and macrophages as predictors of response to bacillus Calmette-Guérin immunotherapy. *Eur Urol* 55: 1386-1395, 2009.
35. Takayama H, Nishimura K, Tsujimura A, Nakai Y, Nakayama M, Aozasa K, Okuyama A and Nonomura N: Increased infiltration of tumor associated macrophages is associated with poor prognosis of bladder carcinoma in situ after intravesical bacillus Calmette-Guerin instillation. *J Urol* 181: 1894-1900, 2009.
36. Tervahartiala M, Taimen P, Mirtti T, Koskinen I, Ecke T, Jalkanen S and Boström PJ: Immunological tumor status may predict response to neoadjuvant chemotherapy and outcome after radical cystectomy in bladder cancer. *Sci Rep* 7: 12682, 2017.
37. Wang X, Ni S, Chen Q, Ma L, Jiao Z, Wang C and Jia G: Bladder cancer cells induce immunosuppression of T cells by supporting PD-L1 expression in tumour macrophages partially through interleukin 10. *Cell Biol Int* 41: 177-186, 2017.
38. Wu SQ, Xu R, Li XF, Zhao XK and Qian BZ: Prognostic roles of tumor associated macrophages in bladder cancer: A system review and meta-analysis. *Oncotarget* 9: 25294-25303, 2018.
39. Maniecki MB, Etzerodt A, Ulhøi BP, Steiniche T, Borre M, Dyrskjøt L, Orntoft TF, Moestrup SK and Møller HJ: Tumor-promoting macrophages induce the expression of the macrophage-specific receptor CD163 in malignant cells. *Int J Cancer* 131: 2320-2331, 2012.
40. Aljabery F, Olsson H, Gimm O, Jahson S and Shabo I: M2-macrophage infiltration and macrophage traits of tumor cells in urinary bladder cancer. *Urol Oncol* 36: 159.e19-159.e26, 2018.
41. Fu H, Zhu Y, Wang Y, Liu Z, Zhang J, Xie H, Fu Q, Dai B, Ye D and Xu J: Identification and validation of stromal immunotype predict survival and benefit from adjuvant chemotherapy in patients with muscle-invasive bladder cancer. *Clin Cancer Res* 24: 3069-3078, 2018.
42. Rubio C, Munera-Maravilla E, Lodewijk I, Suarez-Cabrera C, Karaivanova V, Ruiz-Palomares R, Paramio JM and Dueñas M: Macrophage polarization as a novel weapon in conditioning tumor microenvironment for bladder cancer: Can we turn demons into gods? *Clin Transl Oncol* 21: 391-403, 2019.
43. Pyonteck SM, Akkari L, Schuhmacher AJ, Bowman RL, Sevenich L, Quail DF, Olson OC, Quick ML, Huse JT, Teijeiro V, *et al*: CSF-1R inhibition alters macrophage polarization and blocks glioma progression. *Nat Med* 19: 1264-1272, 2013.
44. Zhu Y, Knolhoff BL, Meyer MA, Nywening TM, West BL, Luo J, Wang-Gillam A, Goedegebuure SP, Linehan DC and DeNardo DG: CSF1/CSF1R blockade reprograms tumor-infiltrating macrophages and improves response to T-cell checkpoint immunotherapy in pancreatic cancer models. *Cancer Res* 74: 5057-5069, 2014.
45. Sica A and Mantovani A: Macrophage plasticity and polarization: In vivo veritas. *J Clin Invest* 122: 787-795, 2012.
46. Bronte V and Murray PJ: Understanding local macrophage phenotypes in disease: Modulating macrophage function to treat cancer. *Nat Med* 21: 117-119, 2015.
47. Wang Q, Hu B, Hu X, Kim H, Squatrito M, Scarpace L, deCarvalho AC, Lyu S, Li P, Li Y, *et al*: Tumor evolution of glioma-intrinsic gene expression subtypes associates with immunological changes in the microenvironment. *Cancer Cell* 32: 42-56.e6, 2017.
48. Rutledge WC, Kong J, Gao J, Gutman DA, Cooper LA, Appin C, Park Y, Scarpace L, Mikkelsen T, Cohen ML, *et al*: Tumor-infiltrating lymphocytes in glioblastoma are associated with specific genomic alterations and related to transcriptional class. *Clin Cancer Res* 19: 4951-4960, 2013.
49. Lin EY, Nguyen AV, Russell RG and Pollard JW: Colony-stimulating factor 1 promotes progression of mammary tumors to malignancy. *J Exp Med* 193: 727-740, 2001.
50. Qian BZ, Li J, Zhang H, Kitamura T, Zhang J, Campion LR, Kaiser EA, Snyder LA and Pollard JW: CCL2 recruits inflammatory monocytes to facilitate breast-tumour metastasis. *Nature* 475: 222-225, 2011.
51. Cortez-Retamozo V, Etzrodt M, Newton A, Ryan R, Pucci F, Sio SW, Kuswanto W, Rauch PJ, Chudnovskiy A, Iwamoto Y, *et al*: Angiotensin II drives the production of tumor-promoting macrophages. *Immunity* 38: 296-308, 2013.
52. Ying W, Tseng A, Chang RC, Morin A, Brehm T, Triff K, Nair V, Zhuang G, Song H, Kanameni S, *et al*: MicroRNA-223 is a crucial mediator of PPAR γ -regulated alternative macrophage activation. *J Clin Invest* 125: 4149-4159, 2015.
53. He X, Tang R, Sun Y, Wang YG, Zhen KY, Zhang DM and Pan WQ: MicroR-146 blocks the activation of M1 macrophage by targeting signal transducer and activator of transcription 1 in hepatic schistosomiasis. *EBioMedicine* 13: 339-347, 2016.
54. Liu Y, Gu Y and Cao X: The exosomes in tumor immunity. *Oncoimmunology* 4: e1027472, 2015.
55. Cooks T, Pateras IS, Jenkins LM, Patel KM, Robles AI, Morris J, Forshev T, Appella E, Gorgoulis VG and Harris CC: Mutant p53 cancers reprogram macrophages to tumor supporting macrophages via exosomal miR-1246. *Nat Commun* 9: 771, 2018.
56. Junker K, Heinzelmann J, Beckham C, Ochiya T and Jenster G: Extracellular vesicles and their role in urologic malignancies. *Eur Urol* 70: 323-331, 2016.



This work is licensed under a Creative Commons Attribution-NonCommercial-NoDerivatives 4.0 International (CC BY-NC-ND 4.0) License.